

Supplemental Materials for

**Integrative Genomics Identified Novel Associations with *APOL1*
Risk Genotypes in Black NEPTUNE Subjects**

Matthew G. Sampson, Catherine C. Robertson, Sebastien Martini, Laura Mariani, Kevin Lemley, Christopher E. Gillies, Edgar A. Otto, Jeffrey B. Kopp, Anne Randolph, Virginia Vega-Warner, Felix Eichinger, Viji Nair, Debbie S. Gipson, Daniel Cattran, Duncan Johnstone, John O'Toole, Serena Bagnasco, Peter Song, Laura Barisoni, Jonathan Troost, Matthias Kretzler, John Sedor, and the Nephrotic Syndrome Study Network

correspondence to: mgsamps@med.umich.edu

This document includes:

Supplemental Tables 1 to 8 (pages 1 to 9)
Supplemental Figures 1 and 2 (pages 10 and 11)
Supplemental Appendices 1 to 5 (pages 12 to 29)
References for Supplemental Appendices (page 30)

Supplemental Table 1. Genotype and allele frequencies for *APOL1* risk alleles in 90 African-American NEPTUNE subjects

Genotype	Cases	Percent
WT* + WT	27	(30)
WT + G1	13	(14)
WT + G2	11	(12)
G1 + G1	13	(14)
G1 + G ⁺ **	2	(2)
G1 + G2	17	(19)
G2 + G2	7	(8)
Total	90	(100)

Risk Allele	Frequency
G1	0.32
G ⁺	0.01
G2	0.23

Number of Risk Alleles	Cases	(%)
0	27	(30)
1	24	(27)
2	39	(43)

*WT = wild type allele

**G⁺ = rare haplotype containing the risk allele at G1^{S342G} but not at G1^{I348M} (Kopp 2011)

Supplemental Table 2. Monogenic SRNS genes sequenced

Dominant	Recessive
<i>ACTN4</i>	<i>COQ2</i>
<i>CD2AP</i>	<i>COQ6</i>
<i>CFH</i>	<i>CUBN</i>
<i>INF2</i>	<i>ITGA3</i>
<i>LMX1B</i>	<i>LAMB2</i>
<i>TRPC6</i>	<i>MYO1E</i>
<i>WT1</i>	<i>NEIL1</i>
	<i>NPHS1</i>
	<i>NPHS2</i>
	<i>PDSS2</i>
	<i>PLCE1</i>
	<i>PTPRO</i>
	<i>SCARB2</i>
	<i>SMARCAL1</i>

Supplemental Table 3. Preterm status and birthweight by *APOL1* risk genotype

	Low-risk	High-risk	Odds Ratio/Beta	p-value
Preterm	11% (5/47)	26% (9/34)	3.0 (0.8,12.7)	0.08
Birthweight (g)	3176 +/- 700 (n=30)	2856 +/- 726 (n=26)	-320(-694,54)	0.10

Birthweight presented as mean +/- SD. P-values and parameter estimates determined using simple linear regression and Fisher's exact test.

Supplemental Table 4-a. Regression analysis of eGFR slope in years adjusting for age, baseline UPC, RAAS blockade, histopathologic diagnosis, and baseline eGFR (n=73)

	$\hat{\beta}$	CI	p-value
HR	-5.3	(-14.1,3.5)	0.24
Age	-0.2	(-0.4,0.1)	0.27
UPC baseline	-0.4	(-1.2,0.3)	0.26
RAAS	-1.9	(-10.9,7.1)	0.68
Histopath			
FSGS	ref	-	-
MCD	9.0	(-2.8,20.9)	0.14
MN	0.9	(-12.6,14.5)	0.89
Other	-6.7	(-17.2,3.8)	0.22
eGFR baseline	-0.2	(-0.4,-0.1)	< 0.01

Supplemental Table 4-b. Regression analysis of eGFR slope in years adjusting only for baseline eGFR (n=73)

	$\hat{\beta}$	CI	p-value
HR	-5.8	(-13.8,2.3)	0.16
eGFR baseline	-0.2	(-0.3,-0.0)	0.01

HR = high-risk genotype
Age = patient age at enrollment
UPC = urine protein to creatinine ratio
RAAS = renin angiotensin aldosterone system blockade
Histopath = histopathologic diagnosis
FSGS = focal segmental glomerulosclerosis
MCD = minimal change disease
MN = membranous nephropathy
Other = other glomerulopathies
eGFR = estimated glomerular filtration rate

Supplemental Table 5-a. Number of patients to ever achieve complete remission and median duration of follow-up by *APOL1* risk status

	Low-risk (n=51)	High-risk (n=39)	p-value
Complete Remission (%)	25 (49)	9 (23)	0.02
Duration follow-up months	22.3 (13.1,29.2)	23.3 (17.2,31.7)	0.38
ESRD or 40% loss of GFR (%)	13 (25)	14 (36)	0.36

Data presented as median (IQR) for quantitative variables and as count (%) for categorical characteristics. P-values determined using Wilcoxon rank-sum test and Fisher's exact test.

Supplemental Table 5-b. Multivariable Cox proportional hazards model of time to first complete remission and *APOL1* risk status

	Hazard Ratio	CI	p-value
HR	0.3	(0.1,0.7)	< 0.01
Age	1.0	(1.0,1.0)	0.40
Histopath			
FSGS	ref	-	-
MCD	3.5	(1.3,9.5)	0.01
MN	0.4	(0.1,2.2)	0.31
Other	0.5	(0.2,1.5)	0.22
UPC baseline	0.9	(0.8,1.0)	< 0.01
eGFR baseline	1.0	(1.0,1.0)	0.64

HR = high-risk genotype

Age = patient age at enrollment

Histopath = histopathologic diagnosis

FSGS = focal segmental glomerulosclerosis

MCD = minimal change disease

MN = membranous nephropathy

Other = other glomerulopathies

UPC = urine protein to creatinine ratio

eGFR = estimated glomerular filtration rate

Supplemental Table 6. Characteristics of subgroups in glomerular and tubulointerstitial gene expression, histomorphometry, interstitial fibrosis and tubular atrophy analyses

	Glomerular Expression			Tubulointerstitial Expression		
	Low-risk (n=29)	High-risk (n=15)	p-value	Low-risk (n=32)	High-risk (n=23)	p-value
Age-yr (median, IQR)	26.0 (13.0,53.0)	17.0 (16.0,18.5)	0.28	29.5 (13.8,53.5)	17.0 (16.0,22.5)	0.17
Pediatric (%)	12 (41)	10 (67)	0.20	12 (38)	14 (61)	0.11
Age of onset-yr	23.0 (11.8,49.0)	17.0 (15.2,17.8)	0.47	24.0 (11.5,50.0)	17.0 (15.0,18.8)	0.32
Duration disease yrs	1.0 (0.0,3.0)	0.0 (0.0,0.8)	0.05	1.0 (0.0,4.0)	0.0 (0.0,1.0)	0.21
Male (%)	22 (76)	10 (67)	0.72	25 (78)	16 (70)	0.54
Histopath (count, %)			0.02			0.01
FSGS	9 (31)	9 (60)		10 (31)	15 (65)	
MCD	8 (28)	2 (13)		8 (25)	3 (13)	
MN	9 (31)	0 (0)		9 (28)	0 (0)	
Other	3 (10)	4 (27)		5 (16)	5 (22)	
Clinical characteristics at baseline						
RAAS blockade (%)	9 (31)	5 (33)	1.00	10 (31)	7 (30)	1.00
eGFR	84.1 (68.4,109.6)	70.2 (59.6,77.4)	0.08	79.8 (57.9,105.3)	70.3 (56.1,80.7)	0.23
UPC	3.0 (2.0,7.7)	2.6 (1.4,5.4)	0.34	3.0 (2.0,7.6)	2.2 (1.1,5.4)	0.24

	Histomorphometry			Interstitial Fibrosis & Tubular Atrophy		
	Low-risk (n=10)	High-risk (n=12)	p-value	Low-risk (n=37)	High-risk (n=26)	p-value
Age-yr (median, IQR)	13.0 (9.8,26.0)	16.5 (15.2,17.2)	0.45	21.0 (12.0,51.0)	17.5 (16.0,39.8)	0.91
Pediatric (%)	7 (70)	9 (75)	1.00	17 (46)	13 (50)	0.80
Age of onset-yr	9.0 (3.2,15.8)	16.0 (14.5,17.0)	0.11	17.0 (9.0,41.0)	17.0 (15.0,26.0)	0.70
Duration disease yrs	0.5 (0.0,4.0)	0.0 (0.0,1.0)	0.57	1.0 (0.0,3.0)	0.5 (0.0,2.8)	0.61
Male (%)	7 (70)	8 (67)	1.00	24 (65)	17 (65)	1.00
Histopath (count, %)			0.12			< 0.01
FSGS	4 (40)	8 (67)		14 (38)	21 (81)	
MCD	5 (50)	2 (17)		12 (32)	2 (8)	
MN	1 (10)	0 (0)		9 (24)	1 (4)	
Other	0 (0)	2 (17)		2 (5)	2 (8)	
Clinical characteristics at baseline						
RAAS blockade (%)	2 (20)	2 (17)	1.00	12 (32)	6 (23)	0.57
eGFR	101.2 (76.1,116.9)	73.7 (64.9,94.9)	0.20	85.7 (65.7,114.1)	68.8 (40.4,88.2)	0.04
UPC	3.2 (1.3,7.7)	2.6 (1.3,5.4)	0.82	3.0 (1.7,6.8)	3.0 (1.3,6.1)	0.90

Data presented as median (IQR) for quantitative variables and as count (%) for categorical characteristics. P-values determined using Wilcoxon rank-sum test or Fisher's exact test.

IQR = interquartile range

Age = patient age at enrollment

Histopath = histopathologic diagnosis

FSGS = focal segmental glomerulosclerosis

MCD = minimal change disease

MN = membranous nephropathy

Other = other glomerulopathies

RAAS = renin angiotensin aldosterone system blockade

eGFR = estimated glomerular filtration rate

UPC = urine protein to creatinine ratio

Supplemental Table 7-a. Histomorphometric correlates by *APOL1* risk status

	Low-risk (n=10)	High-risk (n=12)	p-value
Fractional interstitial area	0.13 +/- 0.05	0.25 +/- 0.07	< 0.01
Average glomerular volume	18979 +/- 6442	17398 +/- 3086	0.49
Cortical glomerular density	2.7e-06 +/- 1.6e-06	1.8e-06 +/- 9.2e-07	0.17

Data presented as mean +/- SD. P-values determined using independent two-sample t-test.

Supplemental Table 7-b. Interstitial fibrosis and tubular atrophy by *APOL1* risk status

	Low-risk (n=37)	High-risk (n=26)	p-value
Interstitial Fibrosis	9.4 +/- 15.7	22.4 +/- 21.7	< 0.01
Tubular Atrophy	10.5 +/- 17.2	23.6 +/- 24.9	0.01

Data presented as mean +/- SD. P-values determined using Wilcoxon rank sum test.

Supplemental Table 8. Top 20 enriched canonical pathways in the low-risk and high-risk *APOL1* co-expression gene sets ranked by statistical significance of overlap

HR-specific canonical pathways

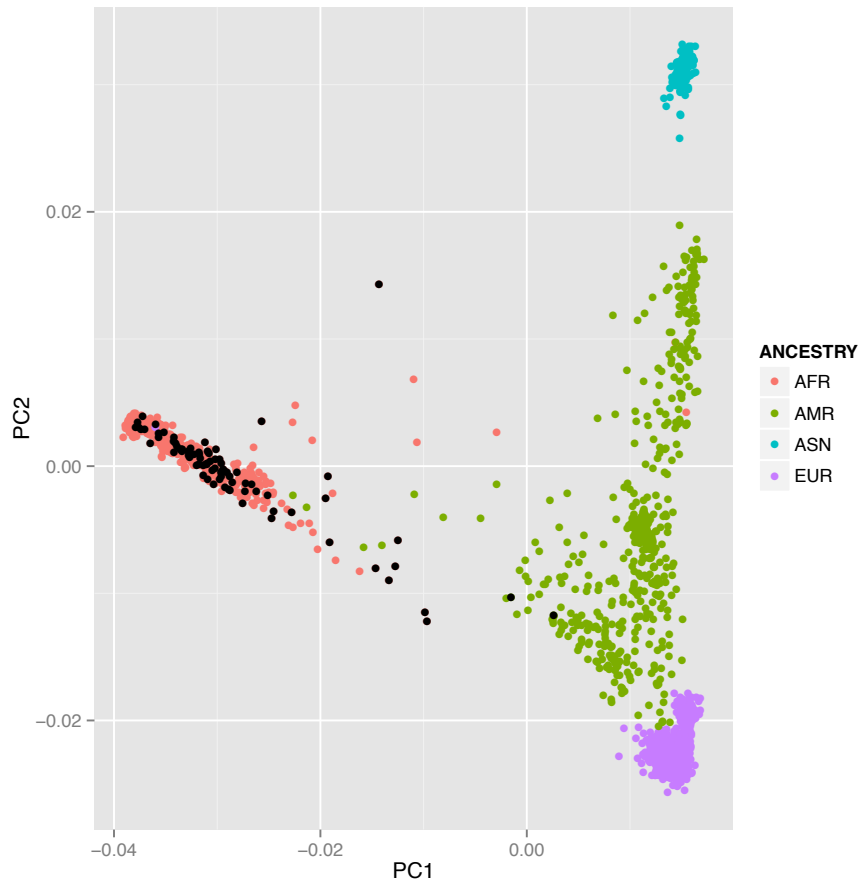
1	Tocopherol Degradation
2	Prostanoid Biosynthesis
3	Intrinsic Prothrombin Activation Pathway
4	Cardiac Hypertrophy Signaling
5	Leukotriene Biosynthesis
6	Proline Degradation
7	Human Embryonic Stem Cell Pluripotency
8	Renin-Angiotensin Signaling
9	Role of JAK family kinases in IL-6-type Cytokine Signaling
10	Antiproliferative Role of TOB in T Cell Signaling
11	ILK Signaling
12	Mineralocorticoid Biosynthesis
13	Activation of IRF by Cytosolic Pattern Recognition Receptors
14	Citrulline Biosynthesis
15	Glucocorticoid Biosynthesis
16	Pancreatic Adenocarcinoma Signaling
17	JAK/Stat Signaling
18	B Cell Activating Factor Signaling
19	Prolactin Signaling
20	Hematopoiesis from Multipotent Stem Cells

LR-specific canonical pathways

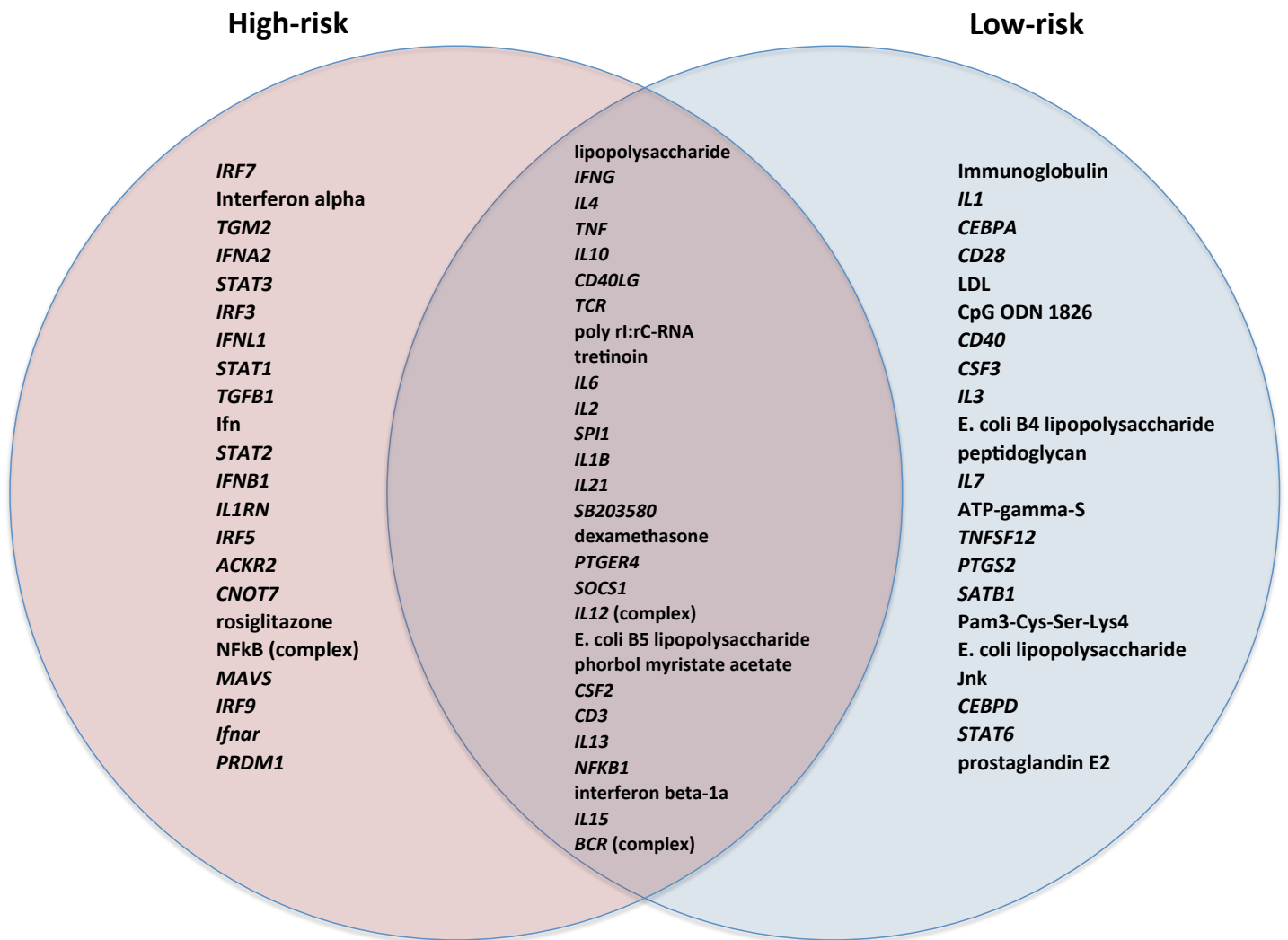
-
-
- 1 Serotonin Degradation
 - 2 Superpathway of Melatonin Degradation
 - 3 Anandamide Degradation
 - 4 Melatonin Degradation II
 - 5 Dopamine Degradation
 - 6 Melatonin Degradation I
 - 7 Thyroid Hormone Metabolism II (via Conjugation and/or Degradation)
 - 8 Retinoate Biosynthesis II
 - 9 Spermine and Spermidine Degradation I
 - 10 NAD Biosynthesis III
 - 11 Nicotine Degradation II
 - 12 Xenobiotic Metabolism Signaling
 - 13 Ceramide Biosynthesis
 - 14 GDP-glucose Biosynthesis
 - 15 Dermatan Sulfate Biosynthesis
 - 16 Glucose and Glucose-1-phosphate Degradation
 - 17 Noradrenaline and Adrenaline Degradation
 - 18 Calcium Transport I
 - 19 Embryonic Stem Cell Differentiation into Cardiac Lineages
 - 20 Methylglyoxal Degradation III
-

Shared canonical pathways

-
-
- 1 Primary Immunodeficiency Signaling
 - 2 Hematopoiesis from Pluripotent Stem Cells
 - 3 Allograft Rejection Signaling
 - 4 B Cell Development
 - 5 Communication between Innate and Adaptive Immune Cells
 - 6 iCOS-iCOSL Signaling in T Helper Cells
 - 7 Systemic Lupus Erythematosus Signaling
 - 8 Role of Pattern Recognition Receptors in Recognition of Bacteria and Viruses
 - 9 Altered T Cell and B Cell Signaling in Rheumatoid Arthritis
 - 10 CD28 Signaling in T Helper Cells
 - 11 Dendritic Cell Maturation
 - 12 Atherosclerosis Signaling
 - 13 Autoimmune Thyroid Disease Signaling
 - 14 Role of NFAT in Regulation of the Immune Response
 - 15 Granulocyte Adhesion and Diapedesis
 - 16 Interferon Signaling
 - 17 OX40 Signaling Pathway
 - 18 Phospholipase C Signaling
 - 19 Agranulocyte Adhesion and Diapedesis
 - 20 CTLA4 Signaling in Cytotoxic T Lymphocytes
-



Supplemental Figure 1. PCA plot of 82 self-reported African-American NEPTUNE subjects. NEPTUNE subjects are represented by black points. 1000 Genomes subjects are colored by ancestry.



Supplemental Figure 2. Predicted upstream transcriptional regulators of the low-risk and high-risk *APOL1* co-expression gene sets

Supplemental Appendix 1: Power calculations for cohort-wide and stratified analyses of eGFR, proteinuria, and complete remission

Due to an absence of analogous preliminary or independent data, we were not able to obtain precise estimates of power that accounted fully for the complexity of the anticipated analyses, including adjustment for multiple covariates and inclusion of interaction terms. However, *a priori* power calculations were performed using simplified models. For all power calculations the type I error (α) was set to 0.05.

Longitudinal eGFR

For the longitudinal analysis of eGFR, we assume that all subjects are followed for five visits (the median number of eGFR and UPC measurements obtained per NEPTUNE subject) and that the standard deviation of eGFR is 22 in the high-risk group and 85 in the low-risk group. These estimates are an approximation of standard deviation based on the median and IQR of eGFR in a previous study of self-reported African Americans with FSGS.¹ Based on these assumptions, we estimated the power for a test of association between eGFR and *APOL1* risk status with 39 high-risk and 51 low-risk subjects using the following equations.

$$z_\beta = \frac{\sqrt{m\delta^2 n_1}}{\sqrt{(\sigma_1^2 + \frac{\sigma_2^2}{r})(1 + (m-1)\rho)}} + z_{\alpha/2}$$

$$r = \frac{n_2}{n_1}$$

$$Power = \Phi(z_\beta)$$

where n_1 and n_2 are sample sizes of the two risk groups, σ_1 and σ_2 are standard deviations of eGFR in the two risk groups, m is the number of visits for each subject, δ is the effect size, ρ is the serial correlation, $z_{\alpha/2}$ and z_β are quantiles of the standard normal distribution, and $\Phi()$ is the cumulative distribution function of the standard normal distribution. Serial correlation (ρ) describes the degree of correlation between measures of eGFR at a given visit with measures of eGFR at other visits.

Using these equations, we computed power for a set of clinically meaningful effect sizes (δ) and across a set of plausible serial correlation values (ρ). The results are presented in **SN Table 1.1**. Our results suggest that we are likely to be modestly underpowered to detect differences in eGFR between risk groups of 25 to 30 ml/min/1.73m². Power calculations generated based on the same assumptions but with only 25 high-risk and 17 low-risk subjects, representing

the sample sizes of an FSGS-only analysis, suggest that we may have substantially limited power to detect associations between eGFR and risk genotypes with effect sizes as large as 30 ml/min/1.73m² (**SN Table 1.2**).

SN Table 1.1 Power of unadjusted GEE analysis of eGFR in all subjects

	$\delta = 15$	$\delta = 20$	$\delta = 25$	$\delta = 30$
$\rho = 0.30$	0.45	0.68	0.86	0.95
$\rho = 0.45$	0.36	0.58	0.77	0.90
$\rho = 0.60$	0.31	0.50	0.69	0.83
$\rho = 0.75$	0.27	0.44	0.61	0.77
$\rho = 0.90$	0.24	0.39	0.56	0.71

SN Table 1.2 Power of unadjusted GEE analysis of eGFR in FSGS subjects

	$\delta = 15$	$\delta = 20$	$\delta = 25$	$\delta = 30$
$\rho = 0.30$	0.19	0.30	0.43	0.57
$\rho = 0.45$	0.16	0.24	0.35	0.48
$\rho = 0.60$	0.14	0.21	0.30	0.41
$\rho = 0.75$	0.12	0.18	0.26	0.36
$\rho = 0.90$	0.11	0.17	0.23	0.32

δ = change in mean eGFR

ρ = serial correlation

Longitudinal UPC

Analogous power calculations were performed for longitudinal analysis of UPC with all of the same assumptions except the standard deviation of \log_2 UPC was assumed to be 1.4 in both groups, which was again an approximation of standard deviation derived from the median and IQR of UPC observed in a previous study.¹ Additionally, for these calculations the effect size was quantified as the percent increase in mean UPC in the high-risk group. Results demonstrate that analysis of all subjects is likely to be well powered to detect a 75% increase and only slightly underpowered to detect a 60% increase in UPC among high-risk subjects, while an FSGS-only analysis is underpowered to detect increases in UPC as large as a 75% (**SN Table 1.3 & 1.4**).

SN Table 1.3 Power of unadjusted GEE analysis of UPC in all subjects

	30%	40%	50%	60%	75%	100%
$\rho = 0.30$	0.48	0.69	0.84	0.93	0.98	1.00
$\rho = 0.45$	0.40	0.59	0.75	0.86	0.95	0.99
$\rho = 0.60$	0.34	0.51	0.66	0.79	0.91	0.98
$\rho = 0.75$	0.29	0.45	0.59	0.72	0.86	0.96
$\rho = 0.90$	0.26	0.40	0.54	0.66	0.81	0.94

SN Table 1.4 Power of unadjusted GEE analysis of UPC in FSGS subjects

	30%	40%	50%	60%	75%	100%
$\rho = 0.30$	0.25	0.38	0.52	0.64	0.79	0.93
$\rho = 0.45$	0.21	0.31	0.43	0.54	0.69	0.86
$\rho = 0.60$	0.18	0.27	0.36	0.46	0.60	0.79
$\rho = 0.75$	0.16	0.23	0.32	0.41	0.54	0.72
$\rho = 0.90$	0.14	0.21	0.28	0.36	0.48	0.66

% = percent increase in UPC

ρ = serial correlation

Complete Remission

To approximate our power to detect an effect of *APOL1* risk genotypes on the time to complete remission, we estimated the median time to complete remission in the low-risk group using the median time to complete remission among NEPTUNE subjects not included in these analyses (i.e. non-black subjects who would not be expected to have *APOL1* risk alleles). The median time to complete remission is equivalent to the earliest time point at which the proportion of complete remission is 50%.² The median time to complete remission was day 573 among non-black subjects. The proportion achieving complete remission never reached 50% among the subset of 85 non-black subjects with FSGS, so we assumed it to be day 1500, which is later than the latest observed follow-up time, in order to approximate power for an FSGS-only analysis. Using these estimates of median time to complete remission, we calculated the approximate power we would have to detect a set of hazard ratios using the following formula for power of a time to event analysis based on exponential survival and accrual.

$$z_{\beta} = \sqrt{\frac{n(\lambda_1 - \lambda_2)^2}{\theta(\lambda_1) + \theta(\lambda_2)}} + z_{\alpha/2}$$

$$\theta(\lambda) = \frac{\lambda^3 t}{\lambda t + e^{-\lambda t} - 1}$$

$$\lambda_1 = -\frac{1}{t_{50}} \ln(0.5)$$

$$h = \frac{\lambda_1}{\lambda_2}$$

$$Power = \Phi(z_\beta)$$

where t is the follow-up time (set to 1329 days, the longest observed follow-up time), λ_1 and λ_2 are the hazard ratios for group 1 and 2, and t_{50} is the median survival time for group 1.

Since the formula used to calculate power requires equal sample sizes in each group, we considered the smallest of the samples sizes of the two risk groups for all subjects (39) and FSGS subjects (17). The hazard ratios that we considered represent a 40% to 75% decrease in the proportion of subjects achieving complete remission for high-risk subjects.

The results presented in **SN Table 1.5** demonstrate that we are well powered to detect hazard ratios of 0.4 when using 39 subjects per group but are underpowered to detect hazard ratios as extreme as 0.25 when studying only 17 subjects per group. The additional 14 and 7 subjects in the low-risk group with all subjects and high-risk group with only FSGS subjects, respectively, will be expected to improve power slightly. However, stratified analyses of the association between time to complete remission and risk group are likely to remain underpowered.

SN Table 1.5 Power for unadjusted Cox regression of complete remission

Hazard Ratio	Power with 39 subjects per group	Power with 17 subjects per group
0.25	0.98	0.63
0.30	0.96	0.51
0.40	0.83	0.33
0.50	0.61	0.20
0.60	0.38	0.13

Supplemental Appendix 2: Results of stratified analyses for eGFR, proteinuria, and complete remission

For reasons related both to our underlying hypothesis and statistical power (as outlined in **Supplemental Appendix 1**), we designed this to be a study of all African-American individuals with proteinuric disease. Here we present analyses of risk genotypes and clinical outcomes stratified by histopathologic diagnosis. Since there is only one high-risk subject with a histopathologic diagnosis of MN (**Table 2**), we have omitted stratified analyses of MN subjects.

Longitudinal eGFR and eGFR slope

In all of the histopathologic groups mean eGFR was lower in high-risk subjects after adjusting for age, UPC, and RAAS blockade use (**SN Table 2.1**). Although not statistically significant, the point estimate for the difference in eGFR between risk groups is potentially clinically meaningful in all three groups considered (-15.2, -14.4, and -18.5 ml/min/1.73m² in FSGS, MCD, and Other cohorts, respectively). The fact that confidence intervals are wide for the estimated difference in mean eGFR between high- and low-risk subjects supports the concept that this stratified analysis lacks statistical power.

SN Table 2.1 GEE analysis of eGFR adjusting for age, baseline UPC, and RAAS blockade, stratified by histopathologic diagnosis

FSGS

	$\hat{\beta}$	CI	p-value
HR	-15.2	(-32.8,2.4)	0.09
Age	-1.1	(-1.5,-0.6)	< 0.01
UPC baseline	-0.2	(-1.7,1.3)	0.79
RAAS	3.8	(-4.7,12.3)	0.38

MCD

	$\hat{\beta}$	CI	p-value
HR	-14.4	(-40.1,11.4)	0.27
Age	-0.5	(-0.8,-0.1)	0.01
UPC baseline	-0.4	(-1.4,0.5)	0.38
RAAS	9.9	(-0.5,20.4)	0.06

Other

	$\hat{\beta}$	CI	p-value
HR	-18.5	(-39.1,2.0)	0.08
Age	-1.2	(-1.9,-0.5)	< 0.01
UPC baseline	1.0	(-2.7,4.7)	0.60
RAAS	-12.6	(-49.3,24.1)	0.50

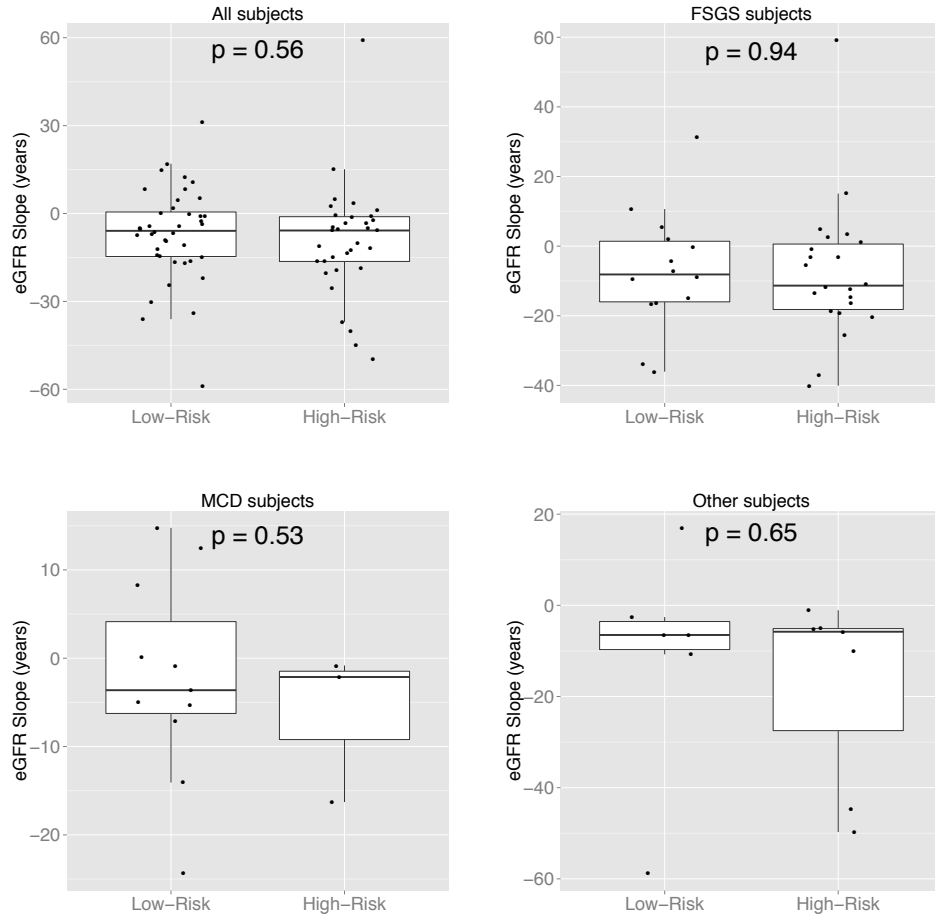
HR = high-risk genotype

Age = patient age at enrollment

UPC = urine protein to creatinine ratio

RAAS = renin angiotensin aldosterone system blockade

As was seen in the combined analysis (**Supplemental Table 4**), in stratified analyses, rate of change in eGFR was not associated with risk genotype (**SN Figure 2.1**) even after adjusting for baseline eGFR (**SN Table 2.2**).



SN Figure 2.1 eGFR slope in years by *APOL1* risk status in all subjects and within histological diagnosis cohorts. P-values determined using independent two-sample t-test.

SN Table 2.2 Regression analysis of eGFR slope in years adjusting for baseline eGFR, stratified by histopathologic diagnosis

FSGS (n=36)

	$\hat{\beta}$	CI	p-value
HR	-1.39	(-20.5,17.7)	0.89
eGFR baseline	-1.63	(-14.9,11.6)	0.81

MCD (n=14)

	$\hat{\beta}$	CI	p-value
HR	20.12	(3.5,36.7)	0.04
eGFR baseline	-4.30	(-15.5,6.9)	0.47

Other (n=13)

	$\hat{\beta}$	CI	p-value
HR	19.92	(-2.3,42.1)	0.11
eGFR baseline	-14.70	(-33.1,3.7)	0.15

HR = high-risk genotype

eGFR = estimated glomerular filtration rate

Longitudinal UPC

Stratified analysis reveals a strong statistical association in between longitudinal UPC and risk genotype among subjects with ‘Other’ histopathologic diagnoses. In the covariate-adjusted analysis of the Other group, the average UPC in high-risk subjects is more than 2.5 times that in low-risk subjects (**SN Table 2.3**). The point estimate within the FSGS group indicates a 41% increase in UPC among high-risk subjects. This is not a statistically significant difference, however, power analysis demonstrates that we are likely underpowered to detect differences with this effect size. Within the MCD cohort, UPC actually decreases slightly in HR subjects, although this is not statistically significant.

SN Table 2.3 GEE analysis of \log_2 UPC adjusting for RAAS blockade and baseline eGFR, stratified by histopathologic diagnosis

FSGS

	$\hat{\beta}$	$2^{\hat{\beta}^*}$	CI	p-value
HR	0.5	1.4	(-0.3,1.3)	0.19
RAAS	-0.8	0.6	(-1.5,-0.1)	0.03
eGFR baseline	-0.0	1.0	(-0.0,-0.0)	0.03

MCD

	$\hat{\beta}$	$2^{\hat{\beta}^*}$	CI	p-value
HR	-0.4	0.8	(-2.1,1.4)	0.68
RAAS	-0.1	0.9	(-1.8,1.6)	0.91
eGFR baseline	0.0	1.0	(-0.0,0.0)	0.98

Other

	$\hat{\beta}$	$2^{\hat{\beta}}$ *	CI	p-value
HR	1.4	2.6	(0.5,2.4)	< 0.01
RAAS	-0.4	0.8	(-1.4,0.6)	0.44
eGFR baseline	-0.0	1.0	(-0.0,0.0)	0.51

* $2^{\hat{\beta}}$ is the factor by which UPC increase in high-risk subjects as compared to low-risk. For example, if $2^{\hat{\beta}}$ is 1.5, average UPC in high-risk subjects is 1.5 times that in low-risk subjects.

HR = high-risk genotype

RAAS = renin angiotensin aldosterone system blockade

eGFR = estimated glomerular filtration rate

Complete Remission

When studying the effect of *APOL1* risk genotypes on time to complete remission stratified by histopathologic diagnosis, we see that the direction of effect is consistent across subgroups. Stratified Cox proportional hazards models were fit for the FSGS and MCD subgroups (SN Table 2.4). Since none of the 8 high-risk subjects in the ‘Other’ subgroup achieved complete remission within the duration of the study (SN Figure 2.2), it was not possible to estimate the effect size or statistical significance of the association through a Cox regression.

In subjects with MCD, at any given time point, high-risk subjects have a lower probability of achieving complete remission as compared to low-risk subjects (HR 0.15, p=0.02). The median time to complete remission was 92 and 192 days for low-risk and high-risk MCD subjects, respectively. While none of the high-risk ‘Other’ subjects achieved complete remission, 6 of the 10 low-risk ‘Other’ subjects did achieve complete remission. The median follow-up time for high- and low-risk ‘Other’ subjects was 774 and 637 days, respectively. The association between complete remission and risk group was not statistically significant within FSGS; however, the point estimate of the effect indicated high-risk FSGS subjects were 60% less likely to achieve complete remission than low-risk FSGS subjects at any given time point.

SN Table 2.4 Cox proportional hazards model of complete remission adjusting for age, baseline UPC and baseline eGFR, stratified by histopathologic diagnosis

FSGS

	Hazard Ratio	CI	p-value
HR	0.38	(0.12,1.21)	0.10
Age	1.02	(0.98,1.05)	0.30
UPC baseline	0.89	(0.71,1.11)	0.29
eGFR baseline	1.03	(1.01,1.05)	< 0.01

MCD

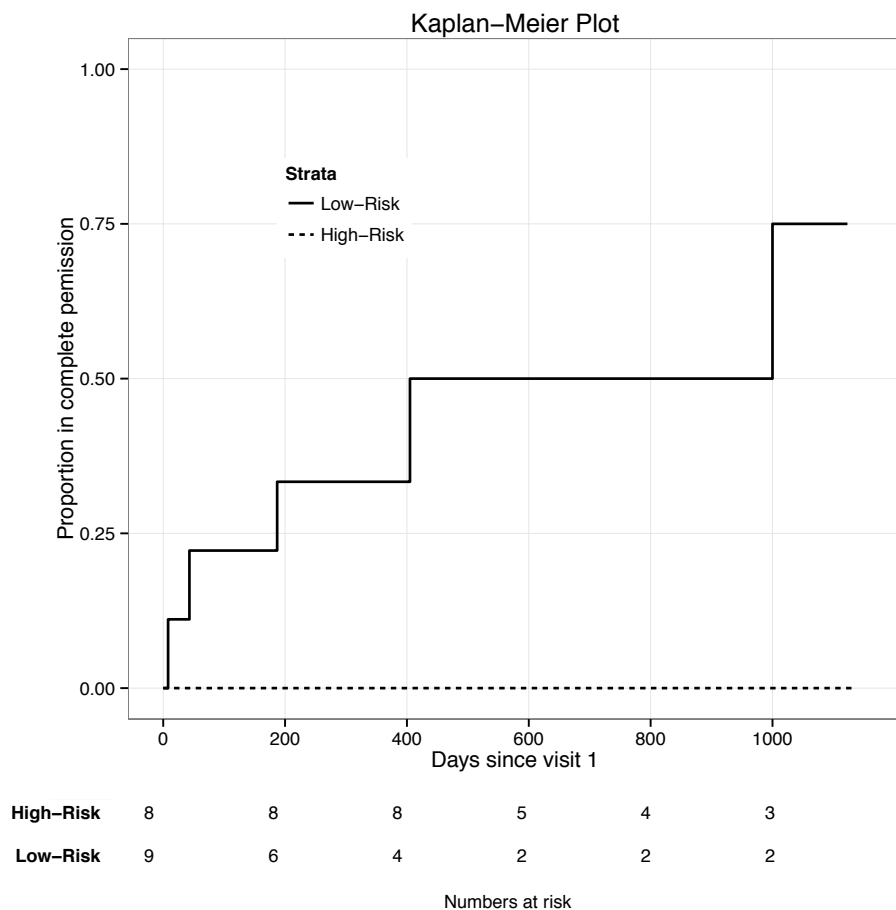
	Hazard Ratio	CI	p-value
HR	0.15	(0.03,0.73)	0.02
Age	0.94	(0.89,1.00)	0.04
UPC baseline	0.76	(0.63,0.92)	< 0.01
eGFR baseline	0.97	(0.94,1.00)	0.03

HR = high-risk genotype

Age = patient age at enrollment

UPC = urine protein to creatinine ratio

eGFR = estimated glomerular filtration rate



SN Figure 2.2 Unadjusted Kaplan-Meier plot of proportion of complete remission among subjects with ‘Other’ histopathologic diagnoses stratified by *APOL1* risk status.

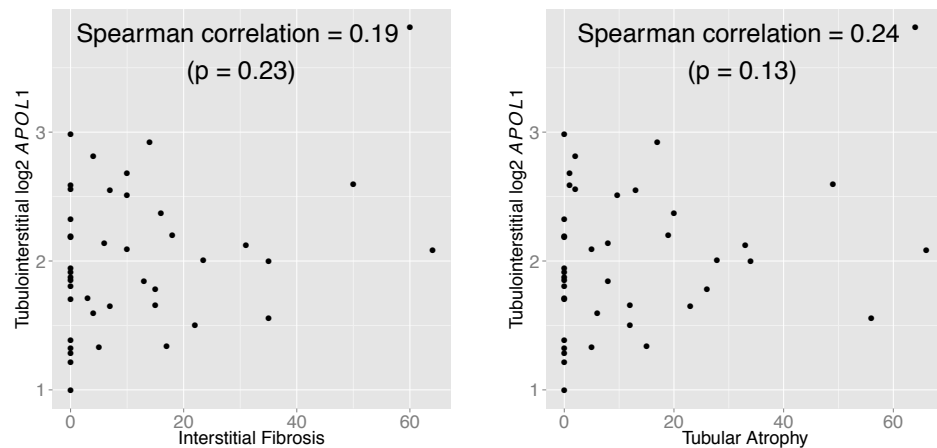
Summary

Each of these stratified analyses is based on a limited number of subjects. Significant parameter estimates may be over estimating effect sizes and non-significant estimates may be the result of underpowered testing. Well-powered follow-up studies will be needed to make any conclusive statements about the relationships between eGFR, UPC, or time to complete remission and risk genotypes within these histopathologic sub-cohorts.

Supplemental Appendix 3: Tubulointerstitial *APOL1* expression and tissue injury

Correlation

Histograms of interstitial fibrosis (IF) and tubular atrophy (TA) revealed severely right-skewed distributions that were not sufficiently remedied via log-transformation. Consequently, the non-parametric Spearman's rank correlation coefficient (ρ) was used to assess the association between *APOL1* expression and tissue injury. Neither IF nor TA was significantly associated with tubulointerstitial (TI) *APOL1* expression (SN Figure 3.1).



Supplemental Figure 3.1 Tubulointerstitial log2 *APOL1* expression versus interstitial fibrosis and tubular atrophy

Confounding

In linear regression models with *APOL1* expression as the response variable, risk genotype is not associated with TI *APOL1* expression even after adjusting for IF or TA (SN Table 3.1 & 3.2).

SN Table 3.2 TI *APOL1* expression vs risk genotype, adjusting for IF (n=42)

	Estimate	Pr(> t)
HR	-0.02	0.93
IF	0.01	0.04

SN Table 3.4 TI *APOL1* expression vs risk genotype, adjusting for TA (n=42)

	Estimate	Pr(> t)
HR	0.01	0.95
TA	0.01	0.07

HR = high-risk genotype

IF = interstitial fibrosis

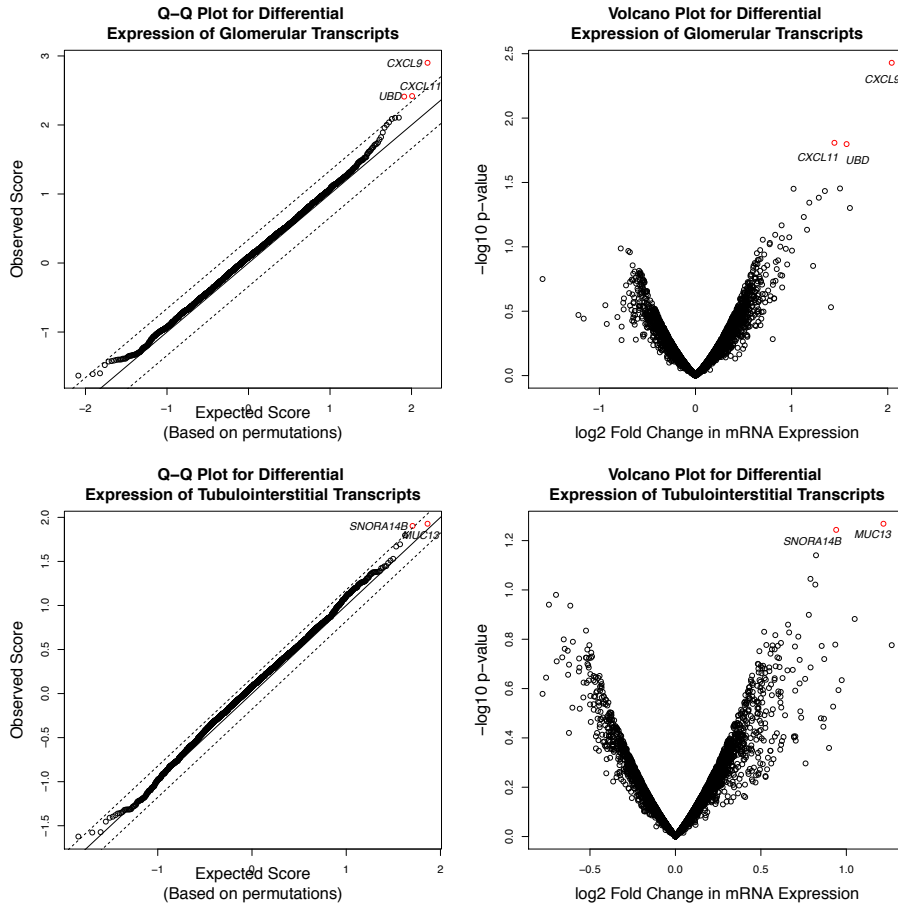
TA = tubular atrophy

Supplemental Appendix 4: Power calculations for genome-wide differential expression analysis

To compute power we have used an approach as described by Wei et al³ in which we provide the ‘pwr.t2n.test’ function from the R package ‘pwr’ with a sample size for each of the groups, an estimate of the standard deviation of gene expression pooled across high- and low-risk groups, the desired statistical power, and the significance threshold.

Since we determined statistical significance for genome-wide differential expression using FDR (a data-dependent approach), for the purpose of power calculations we have used the rather stringent Bonferroni corrected significance threshold ($p < 1.25 \times 10^{-5}$), which corresponds to a family-wise type I error of 0.05. For genes with a pooled standard deviation less than or equal to 0.9, we estimate that we have 80% power to detect fold changes of 3.2 and 2.7 in glomerular and tubular expression, respectively, with the observed sample sizes (15 HR, 29 LR for GLOM; 23 HR, 32 LR for TI). In our observed data, the pooled standard deviation of expression was 0.9 or less for approximately 75% of GLOM genes and 85% of TI genes.

Supplemental Appendix 5: Assessment of genome-wide differential expression analysis



SN Figure 5.1 Summary plots for differential expression analysis of glomerular and tubulointerstitial steady-state mRNA transcript levels. Statistically significant genes are highlighted in red.

Global differential expression, tissue injury, and FSGS

Global analysis of TI *APOL1* identified *MUC13* and *SNORA14B* as significantly differentially expressed between low- and high-risk subjects. To assess whether differential expression of these genes was confounded by IF or TA, linear regressions of expression by genotype adjusting for tissue injury were fit (SN Tables 5.1 & 5.2). While *MUC13* remained significantly differentially expressed at the 0.05 level, *SNORA14B* was no longer significantly differentially

expressed after adjusting for IF or TA. Furthermore, *SNORA14B* was significantly positively correlated with IF and TA independent of risk genotype.

SN Table 5.1 Tubulointerstitial differential expression adjusting for IF (n=42)

Gene Symbol	Risk Genotype p-value	IF p-value
<i>MUC13</i>	0.031	0.662
<i>SNORA14B</i>	0.133	0.022

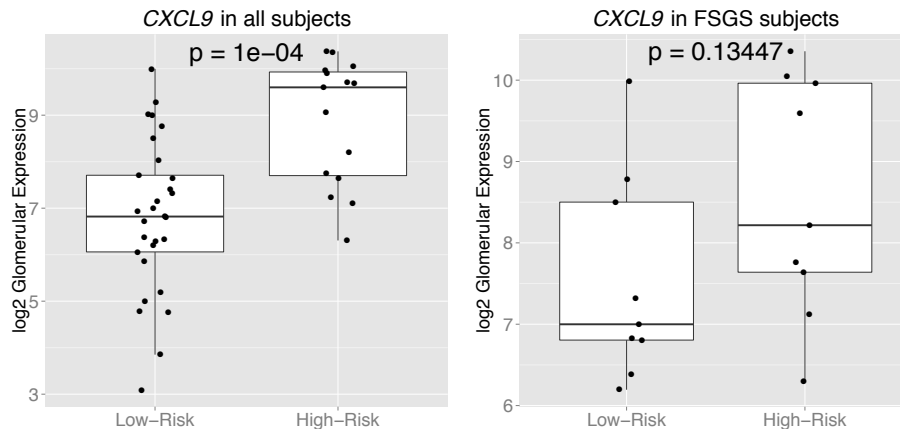
SN Table 5.2 Tubulointerstitial differential expression adjusting for TA (n=42)

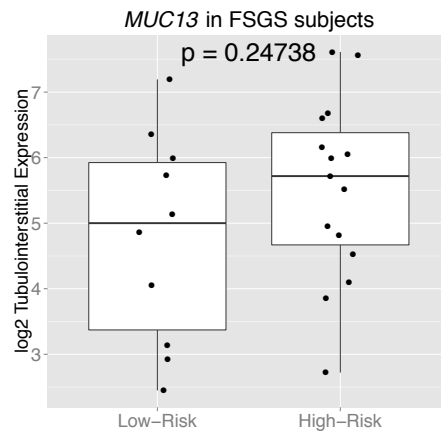
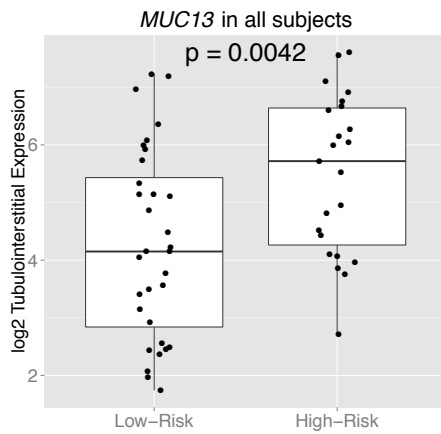
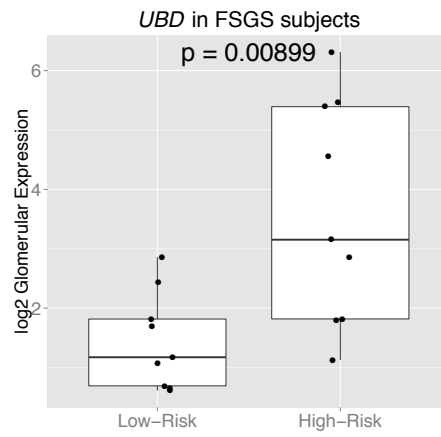
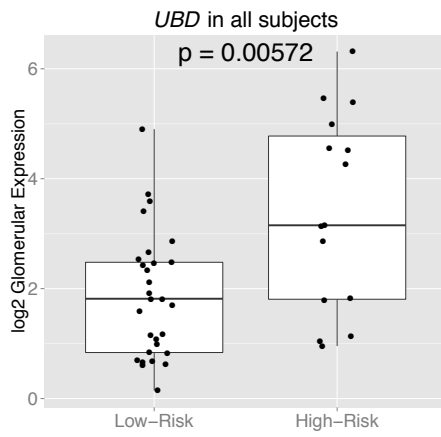
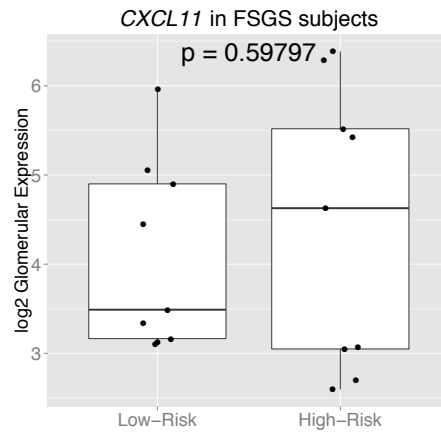
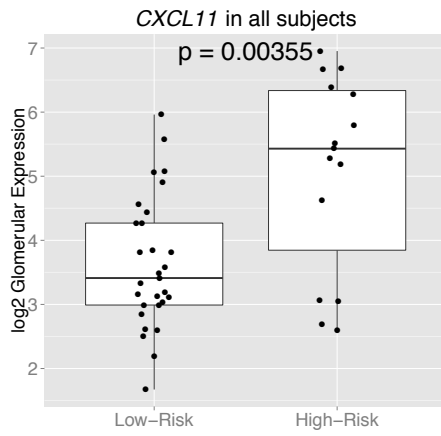
Gene Symbol	Risk Genotype p-value	TA p-value
<i>MUC13</i>	0.028	0.651
<i>SNORA14B</i>	0.097	0.011

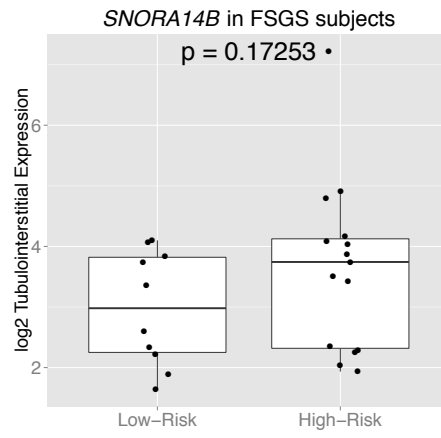
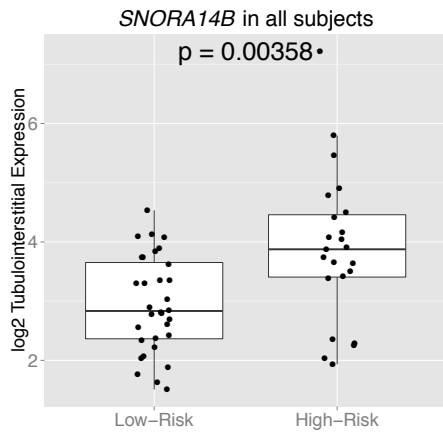
IF = interstitial fibrosis
 TA = tubular atrophy

When examining the five genes found to be differentially expressed in GLOM or TI in only FSGS subjects (**SN Figure 5.2**), they remain upregulated in HR subjects but the strength of association is diminished for the majority of the genes. *UBD* is the only gene that is significantly differentially expressed at the 0.05 level within the FSGS subgroup.

SN Figure 5.2 mRNA expression by *APOL1* risk group for significantly differentially expressed genes







References

- [1] Kopp, J. B. et al. Clinical Features and Histology of Apolipoprotein L1-Associated Nephropathy in the FSGS Clinical Trial. *J Am Soc Nephrol*, doi:10.1681/asn.2013111242 (2015).
- [2] Spruance, S. L., Reid, J. E., Grace, M. & Samore, M. Hazard ratio in clinical trials. *Antimicrobial agents and chemotherapy* 48, 2787-2792, doi:10.1128/aac.48.8.2787-2792.2004 (2004).
- [3] Wei, C., Li, J. & Bumgarner, R. E. Sample size for detecting differentially expressed genes in microarray experiments. *BMC genomics* 5, 87, doi:10.1186/1471-2164-5-87 (2004).